

Supplementary methods

Immunofluorescence analysis

Cells were cultured on Poly-L-lysine coated glass coverslips (BD Bioscience), then incubated with 4% formaldehyde in 10 min, permeabilized in PBS containing 10% goat serum, 3% BSA and 0.2% Triton X-100 for 1 hour, and rinsed in PBS. Slides were incubated with c-myc antibody overnight at 4 °C. To visualize the primary antibody, Cy2-goat anti mouse IgG antibody was incubated with the cells for 1 h at room temperature. DNA was counterstained with Hoechst33258 (Molecular Probes) for 20 min and rinsed in PBS. Samples were mounted in mounting solution (Southern Biotech).

Bisulfite PCR pyrosequencing

All bisulfite-treated DNA polymerase chain reactions (PCR) were performed using HotMaster Mix (Eppendorf, Hamburg, Germany), consisting of HotMaster DNA polymerase and HotMaster Taq Buffer (45 mM KCl, 2.5 mM Mg²⁺, 200 μM dNTP). Since biotin-labeled forward primers were used for PCR amplification, biotin-labeled PCR products could be purified using Sepharose beads and used to generate single-strands for template in the Pyrosequencing reaction, as recommended by the manufacturer, using the Pyrosequencing Vacuum Prep Tool (Pyrosequencing, Inc., Westborough, MA). In brief, the PCR product was bound to streptavidin-coated Sepharose HP (Amersham Biosciences, Uppsala, Sweden), and the Sepharose beads containing the immobilized PCR product were purified, washed, denatured using a 0.2 M NaOH solution, and washed again. Pyrosequencing was performed using the PSQ HS 96 Pyrosequencing System (Biotage, AB, Uppsala, Sweden). Methylation quantification was performed using the software provided. Bisulfite treatment of DNA leads to the formation of a C (methylated) or T (unmethylated) single nucleotide polymorphism that can be quantified by pyrosequencing. Percent methylation was calculated using the ratio of C (methylated)/C+T (methylated+unmethylated).

Figure S1

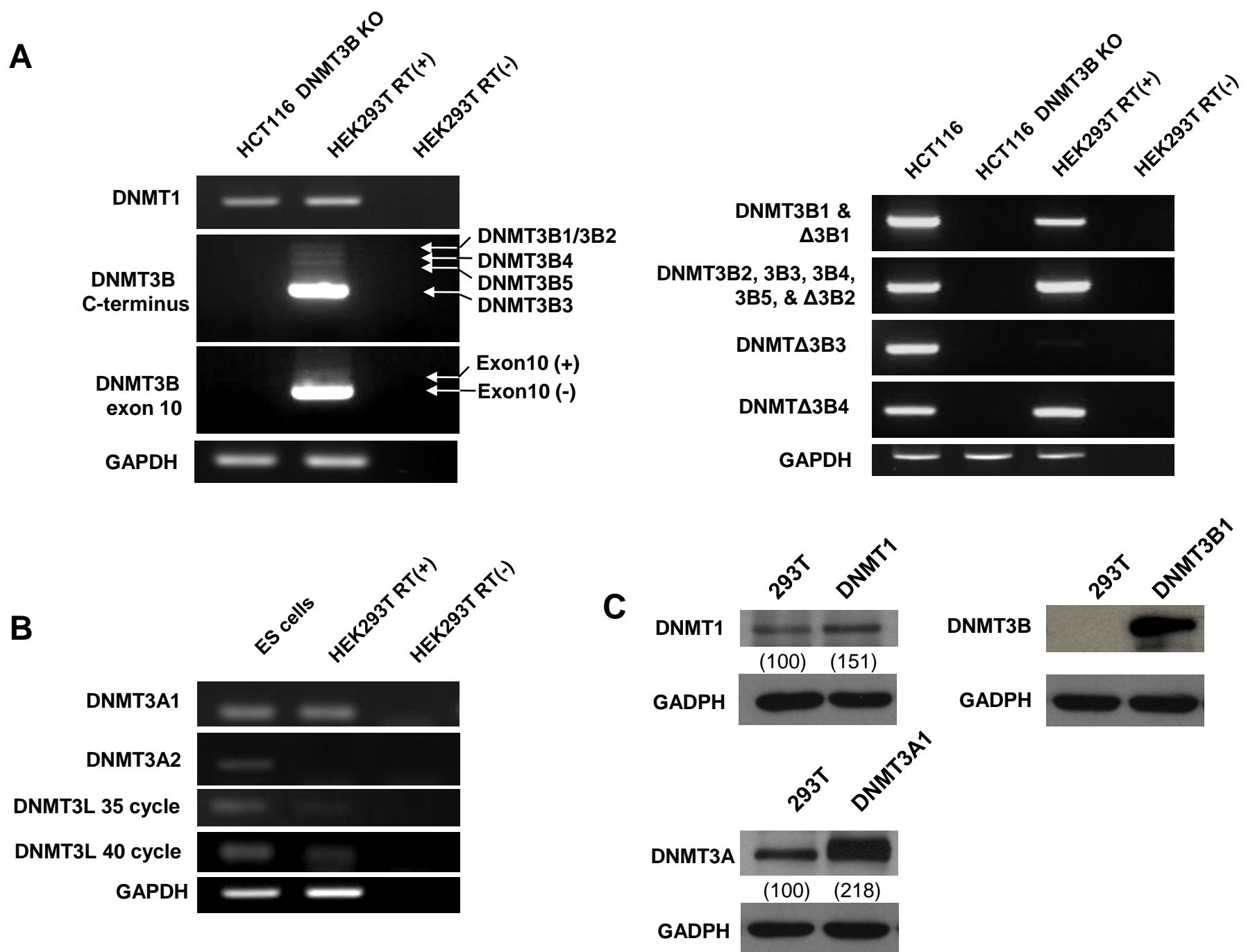


Figure S1. Expression of endogenous DNMTs. (A) Endogenous expression of DNMT3B isoforms. Endogenous expression of DNMT3B isoforms was detected by RT-PCR, as previously described (1). The amplicons obtained for DNMT3B3, DNMT3B4, DNMT3B5, and DNMT3B1/3B2 were of different sizes (left panel). PCR products for DNMT3B1, DNMTΔ3B1, and DNMTΔ3B3 that contained exon10 are indicated as Exon (+). PCR products for DNMT3B isoforms that lacked exon 10 are indicated as Exon (-). DNMT3B1/DNMTΔ3B1, DNMT3B2/DNMTΔ3B2, DNMTΔ3B3, and DNMTΔ3B4 were detected (right panel) as previously described (2), but we could not distinguish DNMTΔ3B1 from DNMT3B1 and DNMTΔ3B2 from DNMT3B2, DNMT3B3, DNMT3B4, and DNMT3B5 due to technical limitations. cDNA from HCT116 and DNMT3B knockout cells (3) were used as positive and negative controls, respectively, for the DNMT3B isoform. (B) Endogenous expression of DNMT3A isoforms and DNMT3L. DNMT3A1 and DNMT3A2 were amplified as previously described (4). DNMT3A1 was detectable, but DNMT3A2 was not detected after 40 PCR amplification cycles. The mRNA expression of DNMT3L was relatively very weak compared to ES cells, but it was detected after 40 PCR amplification cycles. cDNA from human embryonic stem cells was used as a positive control for DNMT3A2 and DNMT3L mRNA expression. (C) Western blot analysis for DNMTs. DNMT expression were detected in HEK293T, DNMT1, DNMT3A1 and DNMT3B1 overexpressed cells using DNMT1 (Imgenex), DNMT3A1 (Abcam), and DNMT3B (NEB). GAPDH expression was used as a loading control. Endogenous DNMT1 and DNMT3A1 were compared with exogenous expression of DNMT1 and DNMT3A1, but endogenous DNMT3B1 could not be detected in HEK293T cells.

Figure S2

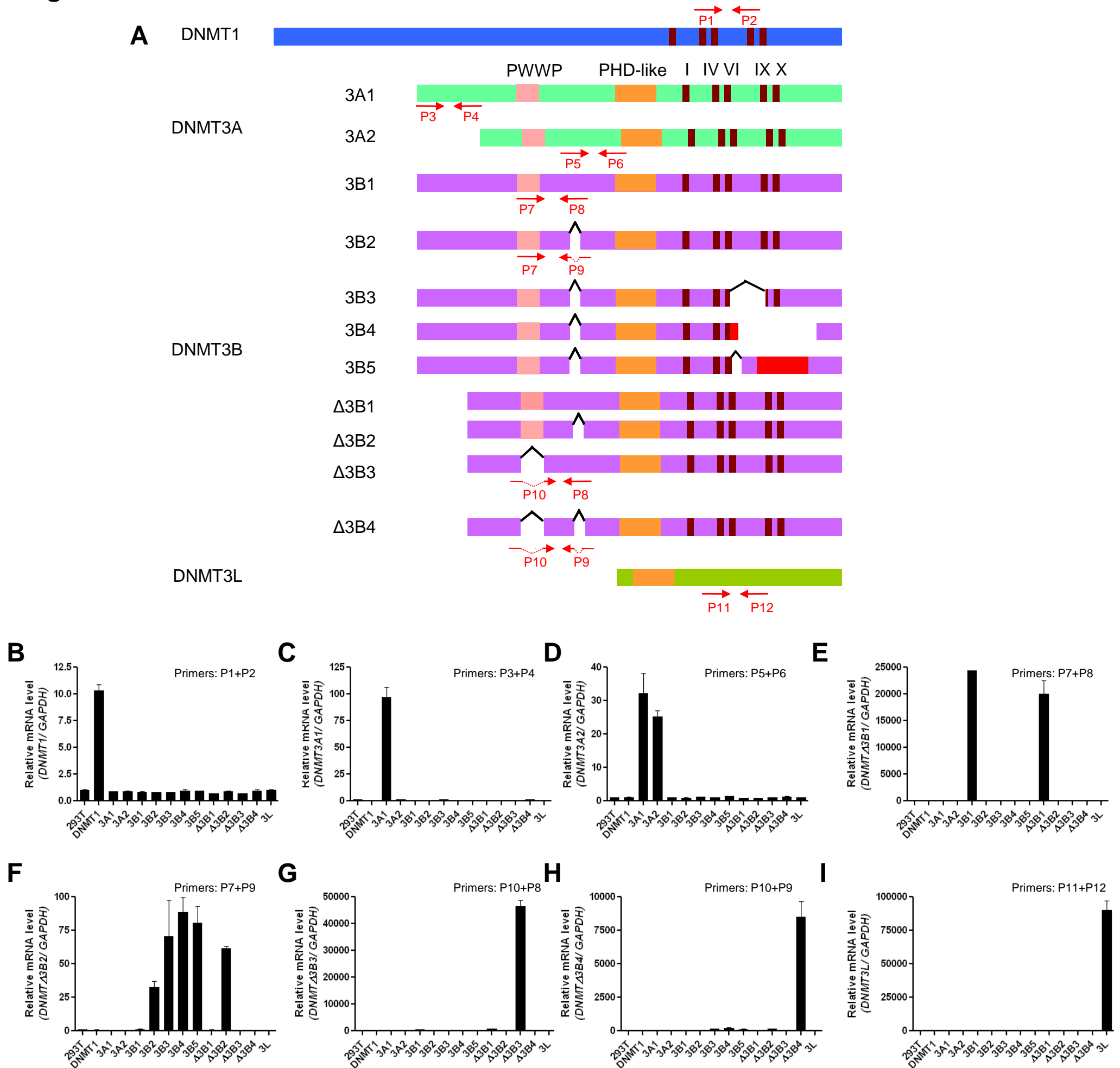


Figure S2. mRNA expression of exogenous DNMTs. (A) Schematic diagram for the location of the primers used for real-time RT-PCR. (B-I) Real-time PCR on mRNA isolated from cells overexpressing each of exogenous DNMTs. The mRNA expression of DNMT1 (B), DNMT 3A1 (C), DNMT3A1 and DNMT3A2 (D), DNMT3B1 and DNMT Δ 3B1 (E), DNMT3B2, DNMT3B3, DNMT3B4, DNMT3B5, and DNMT Δ 3B2 (F), DNMT Δ 3B3 (G), DNMT Δ 3B4 (H), and DNMT3L (I) was assessed with indicated primers (2, 4). Relative mRNA levels are normalized to GAPDH and calculated as fold change relative to control HEK293T cells. Reactions were performed in triplicate, and error bars represent standard deviation.

Figure S3

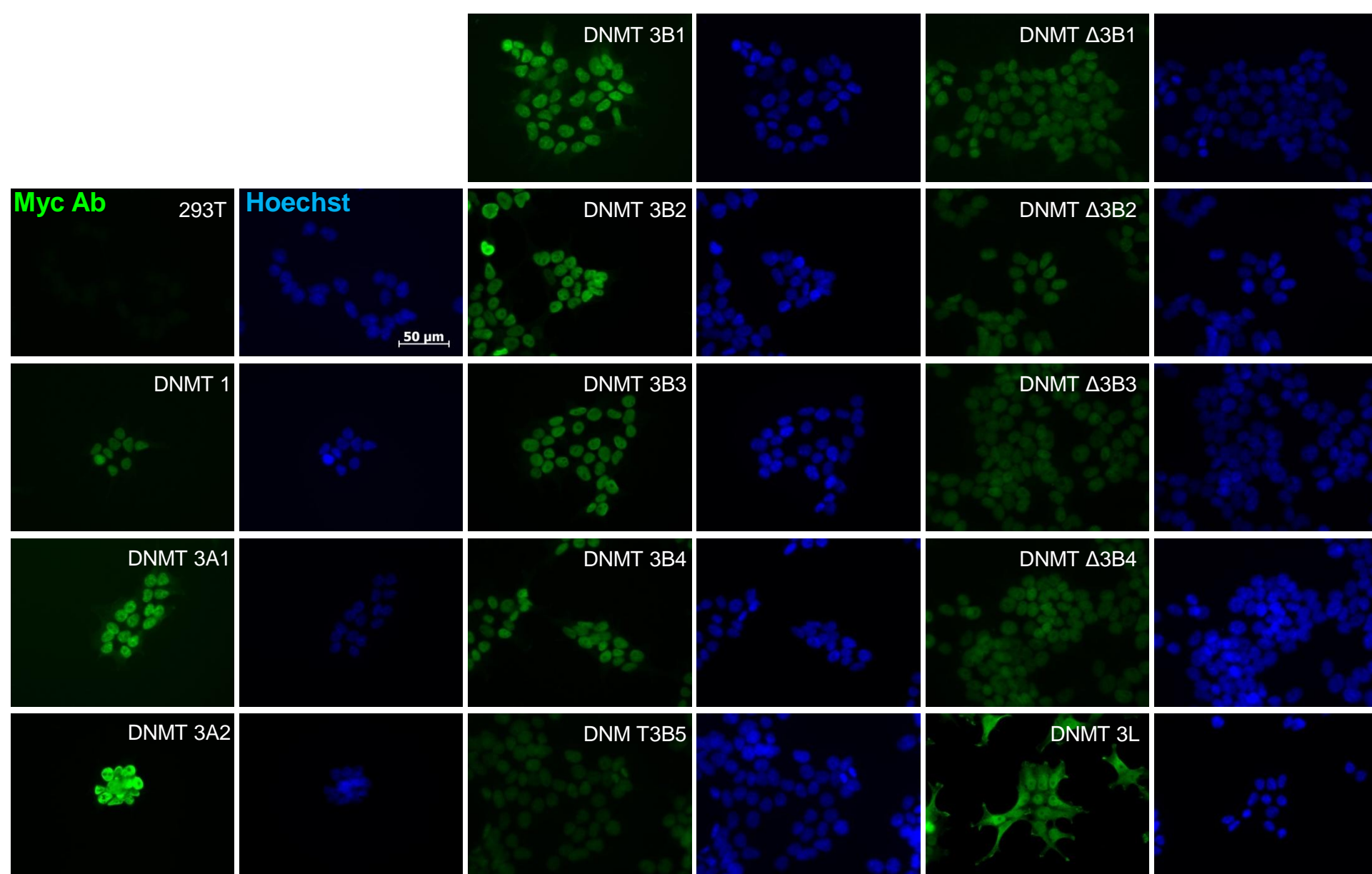


Figure S3. Confirmation of the transfection efficiency of each DNMT. Cell lines stably expressing each N-terminal c-myc-tagged DNMT were immunostained using a c-myc antibody. DNA was counterstained with Hoechst33258. Immunofluorescence images were observed in 400X magnification and scale bar was indicated.

Figure S4

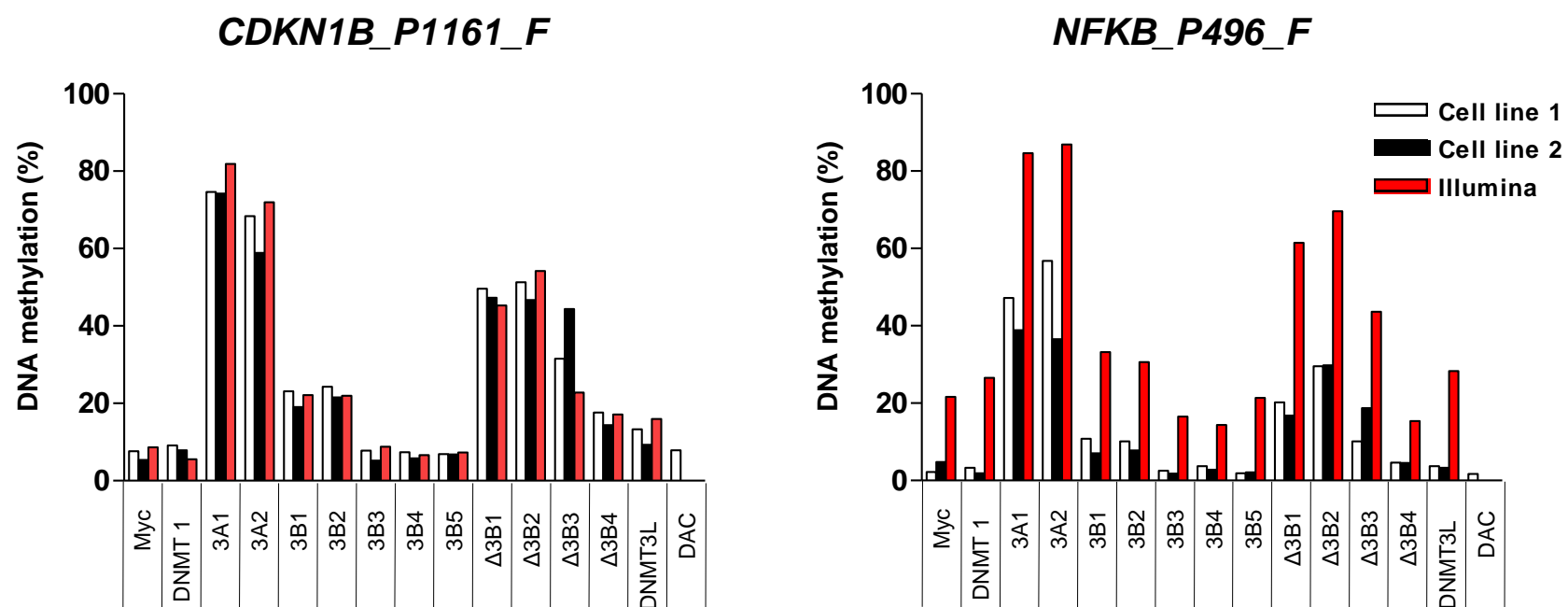


Figure S4. Validation of the Illumina DNA methylation assay using bisulfite PCR pyrosequencing. DNA methylation at the CDKN1B_P1161_F and NFKB_P496_F loci was directly measured by bisulfite PCR pyrosequencing and compared with the percent methylation extrapolated from the β -value in Illumina DNA methylation assay. DNA methylation in HEK 293T cells treated with 5-aza-2'-deoxycytidine, a DNA methylation inhibitor (decreased methylation control), or M.SssI (increased methylation control) is shown as 293T/DAC or 293T/M.SssI, respectively. Two independent stable transfection experiments are indicated as cell line 1 and cell line 2.

Figure S5

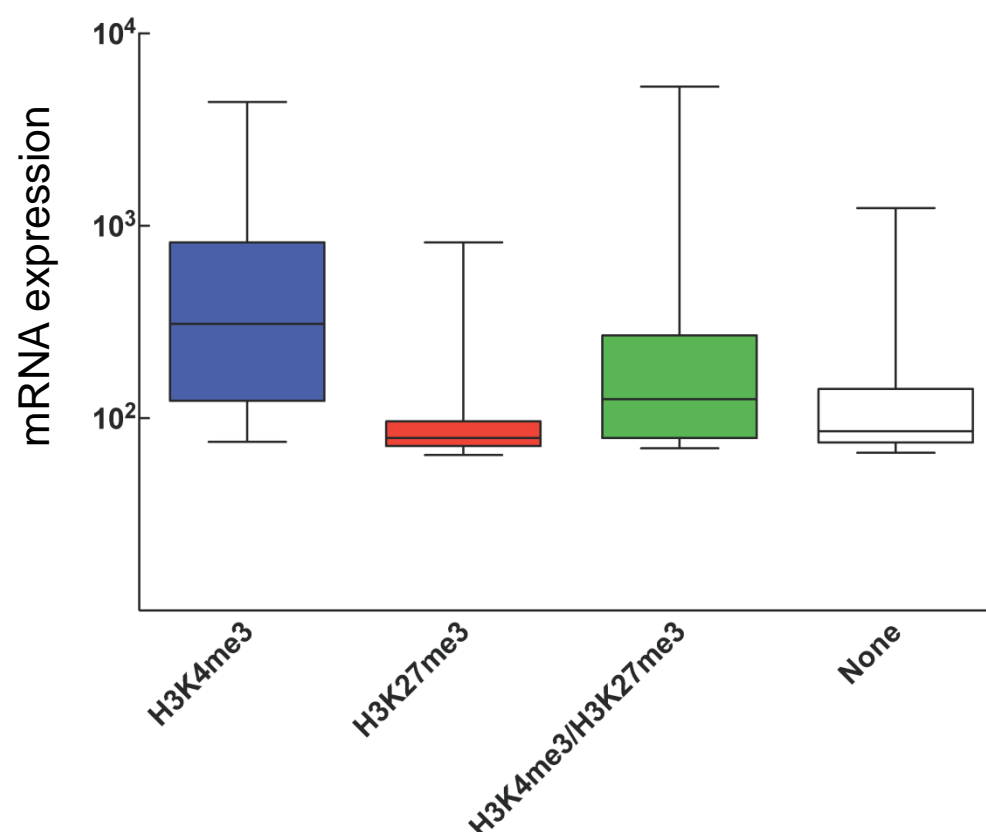


Figure S5. Relationship between transcription and histone mark. Box plot showing 25th, 50th, and 75th percentile expression levels in HEK293T cells for 807 genes studied for DNA methylation that are associated with H3K4me3, H3K27me3, H3K4me3/H3K27me3, and none (neither H3K4me3 nor H3K27me3). Whiskers show 2.5th and 97.5th percentiles. Expression data (y axis) were determined from Illumina expression profiles.

Figure S6

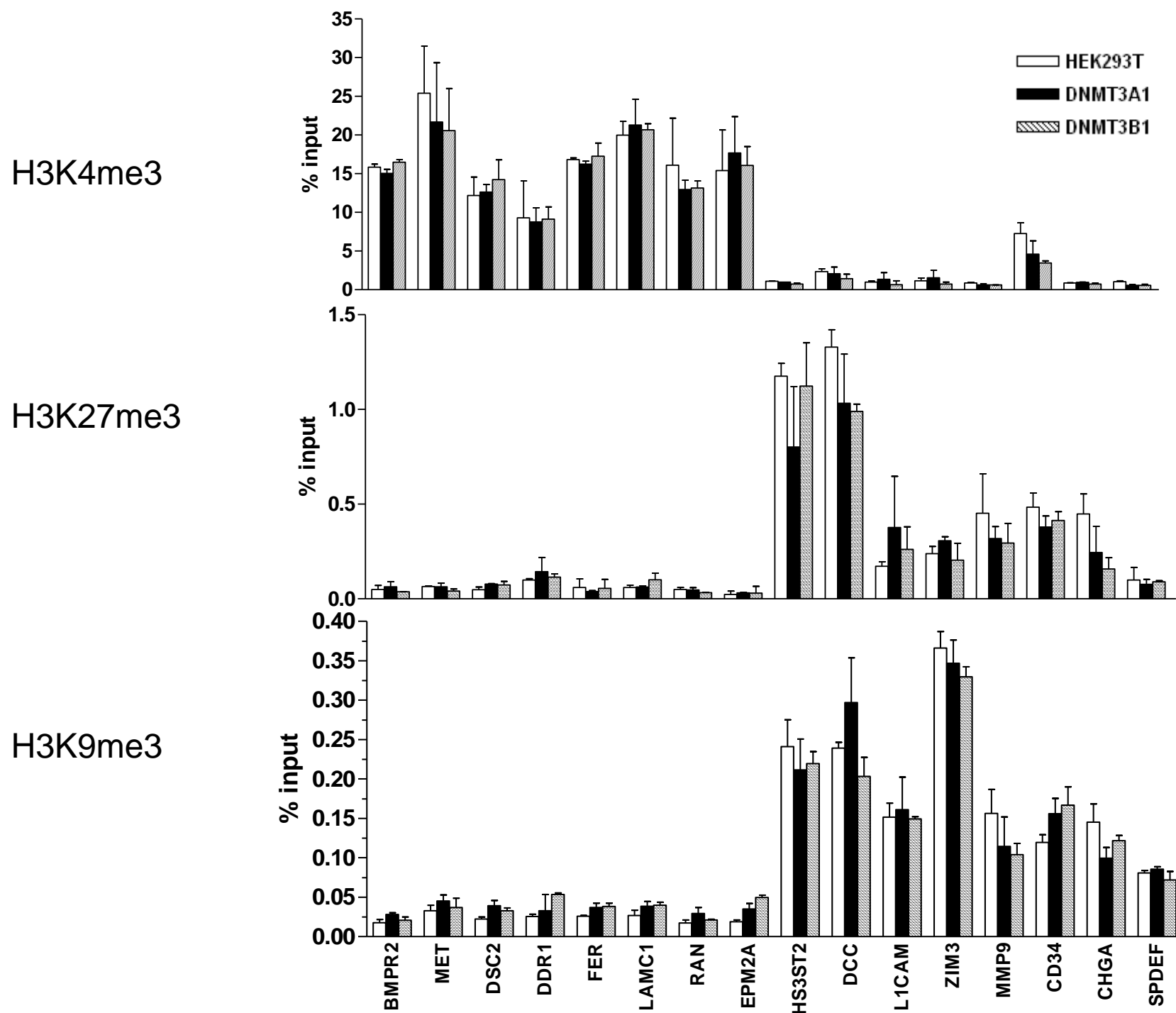


Figure S6. Changes of histone modification in DNA methylated genes. ChIP combined with qPCR to measure histone modifications (H3K4me3, H3K27me3, and H3K9me3) of DNMT3A1 target genes and DNMT3B1 target genes (shown in Figure 5C) in HEK 293T cells (white bar), DNMT3A1 overexpressed cells (black bar), and DNMT3B1 overexpressed cells (striped bar). ChIP data represent the means \pm S.D.

Figure S7

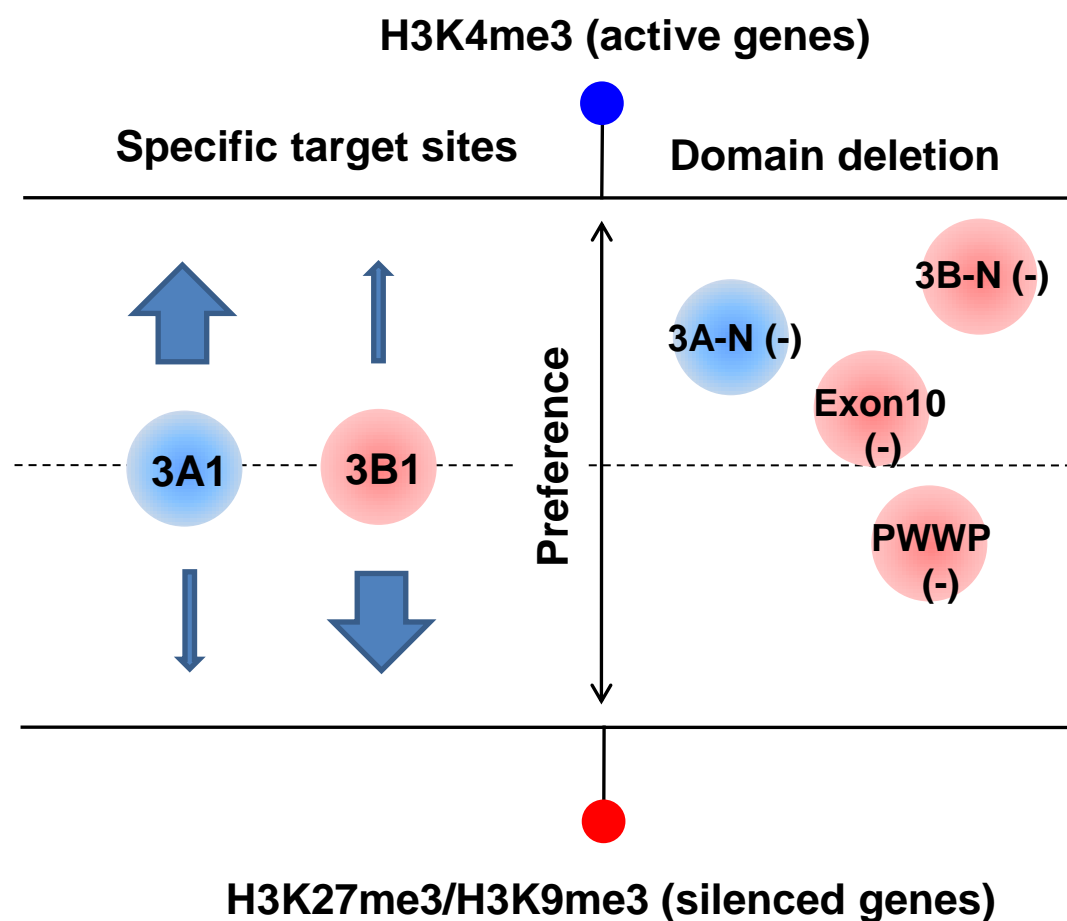


Figure S7. A model for DNMT isoform targeting to H3K4me3 and H3K27me3. Specific target sites for DNMT3A1 were associated with H3K4me3-marked genes, while specific target sites for DNMT 3B1 were associated with H3K27me3-marked genes. The lack of DNMT3B exon10 (Exon10), DNMT3B PWWP (PWWP), DNMT3B N-terminus (3B-N), and DNMT3A N-terminus (3A-N) could change the preferential targets of DNMT isoforms toward H3K4me3 or H3K27me3 histone modifications.

References

1. Robertson, K.D., Uzvolgyi, E., Liang, G., Talmadge, C., Sumegi, J., Gonzales, F.A. and Jones, P.A. (1999) The human DNA methyltransferases (DNMTs) 1, 3a and 3b: coordinate mRNA expression in normal tissues and overexpression in tumors. *Nucleic acids research*, **27**, 2291-2298.
2. Wang, L., Wang, J., Sun, S., Rodriguez, M., Yue, P., Jang, S.J. and Mao, L. (2006) A novel DNMT3B subfamily, DeltaDNMT3B, is the predominant form of DNMT3B in non-small cell lung cancer. *Int J Oncol*, **29**, 201-207.
3. Rhee, I., Bachman, K.E., Park, B.H., Jair, K.W., Yen, R.W., Schuebel, K.E., Cui, H., Feinberg, A.P., Lengauer, C., Kinzler, K.W. *et al.* (2002) DNMT1 and DNMT3b cooperate to silence genes in human cancer cells. *Nature*, **416**, 552-556.
4. Ehrlich, M., Woods, C.B., Yu, M.C., Dubeau, L., Yang, F., Campan, M., Weisenberger, D.J., Long, T., Youn, B., Fiala, E.S. *et al.* (2006) Quantitative analysis of associations between DNA hypermethylation, hypomethylation, and DNMT RNA levels in ovarian tumors. *Oncogene*, **25**, 2636-2645.